Real-Time Harmonic Identification Under Varying Grid Conditions

Evgeniia A. Bulycheva[1], Sergey A.Yanchenko[1]

Abstract: One of the challenges of the power quality management is a need for reliable harmonic identification in grids with multiple non-linear loads. This paper proposes a novel method to accurately determine time-varying harmonic contributions of non-linear loads to the total grid voltage distortion. The use of the invasive measurement approach and ternary pulse sequence as a stimuli guarantees an accurate assessment of harmonic contribution with the account for time-variating harmonic impacts. The application of proposed approach is demonstrated by means of time-domain grid simulation with implemented white-box model of a pulse sequence generator. Statistical estimation of the accuracy of the proposed approach as well as comparison with typical harmonic identification methods justify its effectiveness under non-stationary network conditions.

Keywords: Harmonic identification, Harmonic contribution, Impedance measurement, Non-linear load, Power quality.

1 Introduction

Power quality management is a priority goal in modern electric grids that is currently jeopardized by massive implementation of power electronics devices. In general, improvement of energy efficiency is achieved by introducing sophisticated control of equipment operating modes that in its turn leads to the wide spread of converters featuring nonlinear nature. This leads inevitably to the rise of harmonic voltage distortion, leading to accelerated wear-out of network electrical equipment.

In order to limit the stress of equipment under distorted conditions, harmonic sources should be correctly identified and their impact on the supply voltage should be accurately evaluated. This resulted in the development of numerous methods for assessment of harmonic contributions, which can be roughly divided into two groups: fluctuation [1, 2] and regression methods [3 – 7]. Both groups utilize the measured data representing a variation of network voltages and currents in different operating modes. In order to assure accurate results

---

fluctuation methods require prominent changes of the network operating mode: e.g., turning on/off [1] or variation of the non-linear load [2], energizing of power transformers or switching of power factor correction capacitors [2], etc. Conversely, regression methods determine harmonic contributions based on natural variations of network operating mode implementing statistical analysis [3, 4], state estimation [5, 6] or machine learning techniques [7].

It follows from a more detailed comparison of these methods conducted in [8, 9] that most of them require an accurate representation of the frequency dependent network impedance, which is essential for correct calculation of harmonic contribution. A common practice is to assume that the frequency dependent network impedance is constant over the entire measurement interval. However, network operation generally involves switchings of circuit breakers, transformers and capacitor banks, variation of customer loads, etc. and thus features non-constant grid impedance values. The neglect of these variations may lead to inaccurate evaluation of harmonic contributions.

The present paper addresses the problem of harmonic identification under nonstationary grid conditions by proposing a method that accounts for time-varying frequency response of the network impedance in the real time. This is accomplished by the use of short-term stimuli that allows accurate determination of impedance characteristic with high time discretization. With the known time-varying impedances harmonic contributions of customer and grid can be calculated at each particular time instant according to common procedure [1]. This real-time capability of the proposed method can be useful for harmonic identification in the grid with frequent switchings, low short-circuit capacity or nonlinear customers with nonstationary operating mode.

The remainder of the paper is organized as follows. The general description of the method is provided in Section 2. The model of the pulse sequence generator used for injecting measurement stimuli is described in Section 3. Section 4 presents a grid simulation model with connected stimuli generator used for efficiency assessment of the method. A comparison with typical approaches for harmonic contribution assessment is presented in Section 5. Finally, current results of the research and its future extension are discussed.

2 General Description of the Proposed Approach

2.1 Calculation of harmonic contributions

In order to identify utility and customer harmonic contributions, they are represented in the frequency domain by equivalent Norton models (Fig. 1), including current harmonic sources J_{uh} and J_{ch} in parallel with respective linear harmonic impedances Z_{uh} and Z_{ch}.
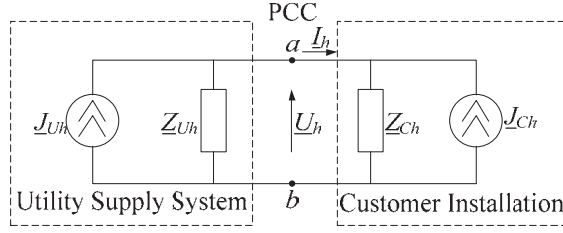
Fig. 1 – *Norton equivalent circuit of the system under study.*

Based on the harmonic voltage U_h and current I_h measured at the point of common coupling (PCC), the utility and customer contributions to voltage distortion at PCC at each harmonic frequency can be determined as follows:

$$\underline{U}_{uh} = (\underline{U}_h - \underline{Z}_{uh}\underline{I}_h)\frac{\underline{Z}_{ch}}{\underline{Z}_{uh} + \underline{Z}_{ch}}, \tag{1}$$

$$\underline{U}_{ch} = (\underline{U}_h + \underline{Z}_{ch}\underline{I}_h)\frac{\underline{Z}_{uh}}{\underline{Z}_{uh} + \underline{Z}_{ch}}. \tag{2}$$

Since U_h and I_h can be measured directly at the PCC, the key problem of assessing the voltage harmonic contribution consists in correct calculation of the utility-and customer-side harmonic impedances Z_{uh} and Z_{ch}. This can be done by measuring the response of the system to the generated stimuli according to the invasive measurement approach. In this case, network is represented as a voltage harmonic source U_{uh} in series with linear harmonic impedance Z_{uh}. A pulse sequence generator connected to the network is represented as a current harmonic source J_{nh} with wide spectrum (Fig. 2).
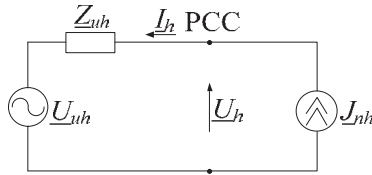

Fig. 2 – *Equivalent circuit of network with pulse sequence generator.*

When using the harmonic current source, it is possible to eliminate the error due to preexisting harmonics by taking them into account. The harmonic impedance $\underline{Z}_{uh}$ is then given by:

$$\underline{Z}_{uh} = \frac{\underline{U}_{2h} - \underline{U}_{1h}}{\underline{I}_{2h} - \underline{I}_{1h}}, \tag{3}$$

where $\underline{U}_{1h}$, $\underline{U}_{2h}$, $\underline{I}_{1h}$, $\underline{I}_{2h}$ – voltages and currents before and after connecting harmonic current source.

In order to eliminate the impact of preexisting grid harmonics impedance characteristic can be defined in accordance with (4) on the basis of interharmonic components of voltage and current produced by injected stimuli [2]:

$$\underline{Z}_h = \frac{\underline{U}_h}{\underline{I}_h},$$ (4)

assuming that no interharmonic components were present in the network prior to the injection.

Then, the harmonic impedance is calculated as the mean of two adjacent interharmonics:

$$\underline{Z}_{uh} = \frac{\underline{Z}_{h-1} + \underline{Z}_{h+1}}{2}.$$ (5)

2.2 Ternary pulse sequence

Utility and customer impedance identification is produced by injection of a ternary pulse sequence (Fig. 3a), that features various benefits if used as a measurement stimuli [10 – 13], e.g.:

– wide almost uniform harmonic spectrum (Fig.3b);

– ability to adjust the spectrum in accordance with the studied network by eliminating certain harmonic orders;

– high immunity against grid original distortion;

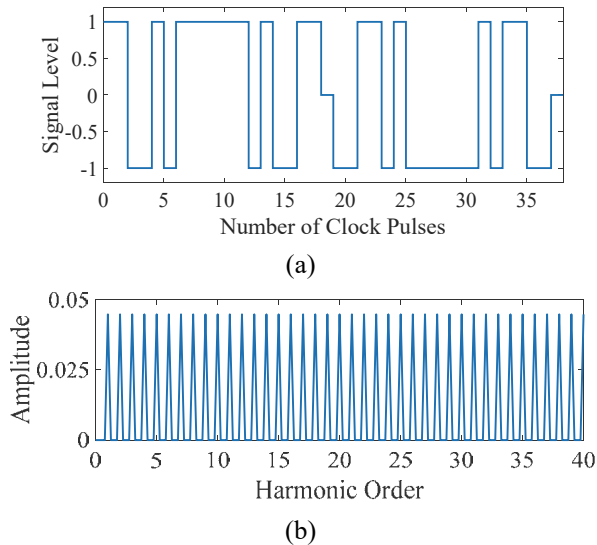– low impact on the grid operating mode.

(a)

(b)

Fig. 3 – (a) *Three-levels of the ternary pulse sequence;*
(b) *Spectrum of the ternary pulse sequence.*

Ternary pulse sequences consist of bit streams of ±1 and 0 occurring in a predefined manner. Low amplitude of the pulses guarantees negligible impact on the grid equipment and at the same time high resilience against noise due to the energy uniformly distributed along the signal spectrum.

Furthermore, the prominence of the ternary pulse sequences can be improved in the case of low signal-to-noise ratio by easily adjusting its length or amplitude, thus, providing accurate results in non-ideal noisy conditions.

A Matlab-based package *prs* [14] is used in the current research for generating the signal of the ternary pulse sequence. This allows to tune its parameters in accordance with the short circuit power and structure of the network and types of connected non-linear loads.

2.3 Structure of the method for harmonic identification

The structure of the proposed method for real-time harmonic identification is shown in the flow chart in Fig. 4.
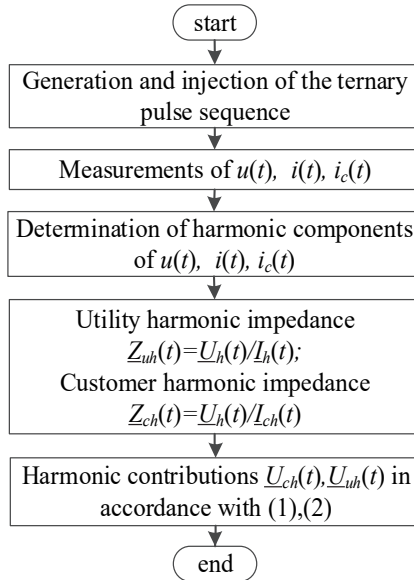

Fig. 4 – *Flow chart of the proposed approach.*

First, multiple injections of ternary pulse sequences corresponding to the studied time interval are generated at the PCC. Then, resulting voltage $u(t)$ and current $i(t)$ waveforms are measured and decomposed with the short-term Fourier transform in order to acquire voltage $U_h(t)$ and current $I_h(t)$ harmonics in the time-frequency domain. A ratio of time-dependent voltage harmonics at the PCC $U_h(t)$ to the magnitude of the spectrum of the ternary sequence $I_h(t)$ represents time variation of grid harmonic impedance $Z_{uh}(t)$. Similarly, customer harmonic

impedance is calculated as a ratio of harmonic voltage $U_h(t)$ to customer harmonic current $I_{ch}(t)$. These are eventually, used to calculate the variation of harmonic contributions according to (1) and (2).

3   Modeling Pulse Sequence Generator

As mentioned previously parameters of the ternary pulse sequence determine the accuracy of measured impedances and consequently harmonic contributions. Hereafter, a more detailed insight in the stimuli generation process is provided by considering the operation of the pulse sequence generator. The respective white-box Simulink-based model presents a single-phase voltage-source inverter [15, 16] with the control system determining the parameters of stimuli.

The model of the pulse sequence generator contains two main parts:

– Power plant including constant power source, DC capacitor, full bridge inverter and input LCL-filter (Fig. 5);
– Control part containing phase-locked-loop (PLL), voltage and current control loops and pulse width modulation (PWM) block (Fig.6).
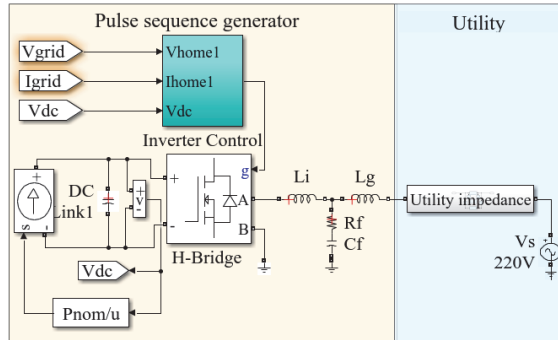

Fig. 5 – *Grid simulation model with connected pulse sequence generator.*
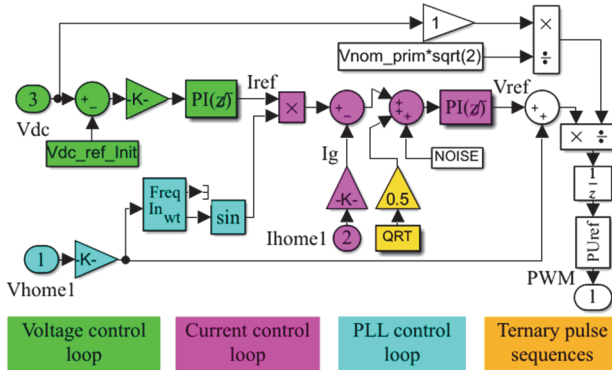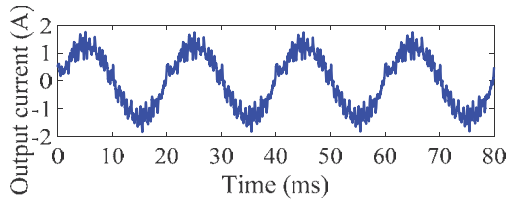

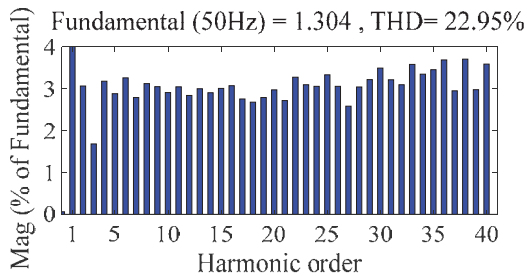**Fig. 6** – *Control structure of the pulse sequence generator.*

The pulse sequence generator parameters are presented in the **Table 1**. A ternary pulse sequence generated with *prs* package is added to the reference current of the inverter thus a measurement stimuli is injected into the studied grid. Resulting output current waveform and its spectrum are presented in Figs. 7a and Fig. 7b respectively. It follows from the figures, that with relatively low level of disturbance, wide and uniform spectrum of the stimuli is produced that allows clear identification of high-order components of impedance characteristic.

Table 1

Parameters of a Pulse Sequence Generator.

LCL-FILTER							
L_i [mH]		L_g [mH]			C_f [uF]		R_f [Ω]
7.292		5.728			1.97		50
PULSE SEQUENCE GENERATOR							
DC-link		PLL			PI voltage control		PI current control
V_{DC} [V]	C_0 [uF]	K_{Ppll}	K_{Ipll} [s⁻¹]	K_{dpll}	K_{Pv}	K_{Iv} [s⁻¹]	K_{Pi}	K_{Ii} [s⁻¹]
450	1500	180	3200	1	30	200	0.35	1
V_{AC} [V]		PWM frequency [Hz]			Rated power [W]		Length of the pulse sequence
220		20 000			200		1009-bit

(a)

Fundamental (50Hz) = 1.304 , THD= 22.95%

(b)

Fig. 7 – (a) *The waveform of the injected stimuli;*
(b) *The spectrum of the injected stimuli.*

Fig. 8 depicts a frequency-dependent input impedance of the pulse sequence generator that justifies its negligible impact on the assessment of resulting harmonic contributions. The contribution of the pulse sequence generator to the total voltage distortion U_{ch} can be estimated by considering it as a customer according to (2). Taking into account that the generator impedance Z_{inv} is much higher than the utility impedance Z_{uh} (Fig. 8) equation (2) can be simplified to:

$$\underline{U}_{ch}(t) = \underline{Z}_{uh}\underline{I}_h(t) . \tag{6}$$

The values of both stimuli spectrum I_h and network impedance Z_{uh} are quite low in respect to customer and utility harmonic contributions resulting in negligible impact of the pulse sequence generator on the calculation accuracy. This is further justified by statistical accuracy assessment provided in the following section.
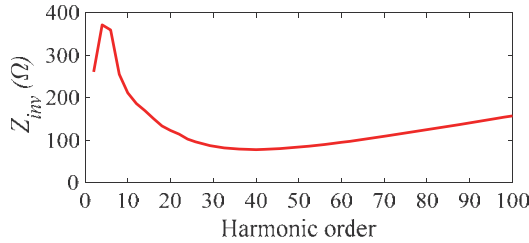

Fig. 8 – *Frequency dependent input impedance of the pulse sequence generator.*

4   Simulation Verification

In this section the use of the proposed approach for harmonic identification is demonstrated under varying grid and load conditions. Statistical estimation of the accuracy reveals good capability of the method to correctly reproduce non-stationary harmonic contributions of utility and customer.

4.1   Online measurements and experimental verification

A grid simulation model used for application of the method is presented in Fig. 9. A varying nonlinear load is represented by two sets of switchable harmonic current sources of the 5th, 7th, 11th and 13th orders in parallel with resistors *Rn1*, *Rn2* corresponding to the load at fundamental frequency. A grid impedance variation is represented by several switchable sets of resistors *R1*, *R2*, *R3* and inductors *L1*, *L2*, *L3*. Finally, nonstationary levels of network distortion are implemented by the switch connecting voltage harmonic sources. During the measurement period a sequence of switchings is performed in order to produce nonstationary harmonic contributions of utility and customer.

The impedance characteristic at each time instant was calculated based on the interharmonic multiples of 12.5 Hz corresponding to the 4 excitation periods

of the injected pulse sequence. Multiple injections of ternary pulse sequences covering the whole measurement interval provide the time characteristic of utility and customer harmonic impedances that are further used to calculate their respective harmonic contributions in accordance with (1) and (2).
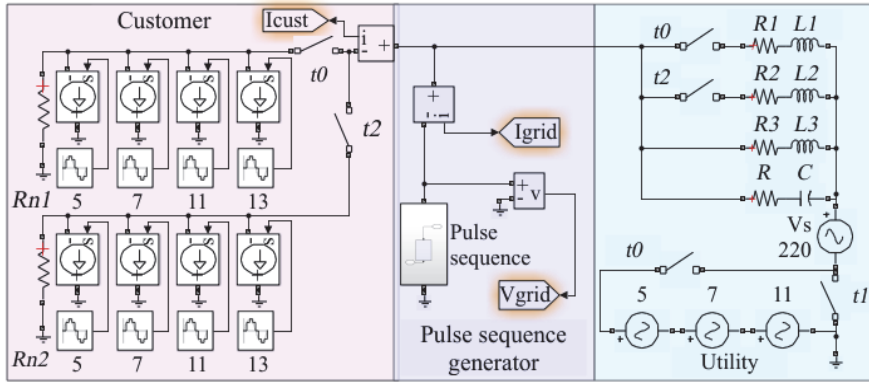

Fig. 9 – *Grid simulation model.*

A model of Fig. 9 was simulated multiple times with randomly varying impedance values and switching instants providing voltage and current data that were further used for determining time-frequency impedances and harmonic contributions of utility and customer (exemplarily depicted in Figs. 10 and 11).
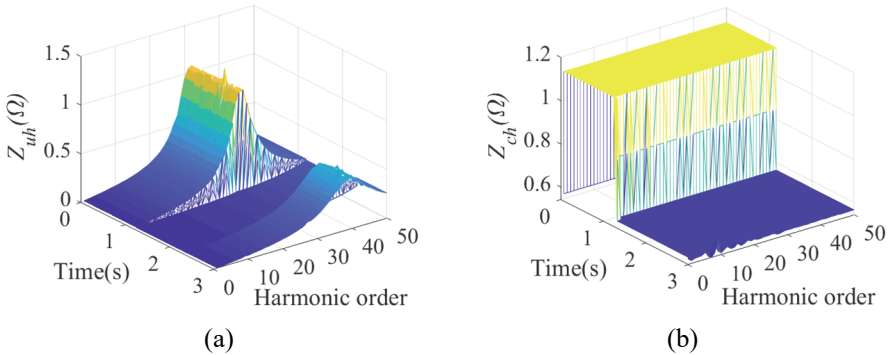

(a) (b)

Fig. 10 – (a) *Time-frequency impedance of the utility;*
(b) *Time-frequency impedance of the customer.*

Variation of the grid impedance leads to the rise of resonant conditions at particular frequencies (Fig. 10a). Fig. 10b depicts the decrease of the customer impedance at fundamental frequency and, consequently, increase of the load. Fig. 11a presents a variation of the utility contribution for particular harmonics that is affected by both varying original grid distortion and occurrence of network resonant conditions. The behavior of customer harmonic contribution in Fig. 11b

is affected not only by its operating mode but also by changing network impedance.
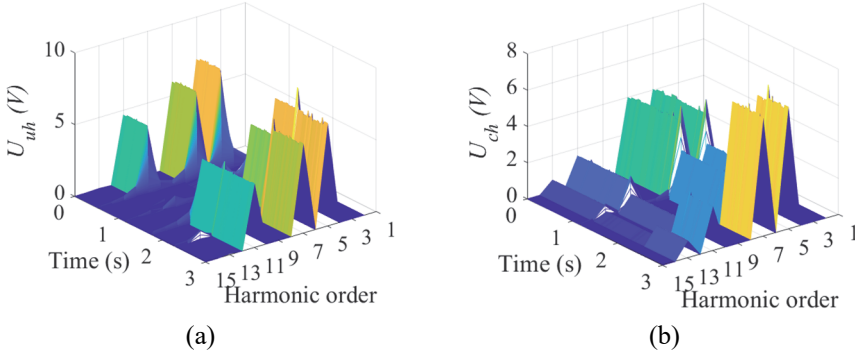

(a)　　　　　　　　　　　　　(b)

Fig. 11 – (a) *Time varying harmonic contribution of the utility;*
(b) *Time-varying harmonic contribution of the customer.*

Multiple simulations (appr. 50) conducted with the described model allowed statistical assessment of the accuracy of the developed method. For each simulation the impedance profile and voltage contribution plots at particular harmonic frequencies were compared with corresponding references by calculating the correlation coefficient ρ:

$$\rho = \frac{\sigma_{xy}}{\sigma_x \sigma_y} = \frac{\displaystyle\sum_{i=1}^{n}(x_i - \overline{x})(y_i - \overline{y})}{\sqrt{\displaystyle\sum_{i=1}^{n}(x_i - \overline{x})^2 \sum_{i=1}^{n}(y_i - \overline{y})^2}} , \tag{7}$$

where x and y are calculated and reference values; σ_x and σ_y are the variance of x and y; σ_{xy} is the covariance between and x and y; $\overline{x}$ and $\overline{y}$ are the mean values of x and y.

The closeness of the correlation coefficient to 1 testifies the degree of match between calculated and reference characteristics. Resulting plots showing the distribution of the correlation coefficient for the utility impedance ρ_{Zuh} and the customer impedance ρ_{Zch} up to the 50th harmonic are provided in Fig. 12 and Fig. 13. Fig. 14 presents a distribution of the correlation coefficient for utility ρ_{Uuh} (Fig. 14a) and customer ρ_{Uch} (Fig. 14b) harmonic contributions at particular harmonic frequencies. It follows from the figures that good convergence level with the reference data is achieved by the proposed method. In 95% of cases, the values of the correlation coefficients for the utility impedance and the customer impedance are greater than 0.97 and 0.9992, respectively. Similarly, values of the correlation coefficients for the utility and customer harmonic contributions are greater than 0.993 and 0.94, respectively.
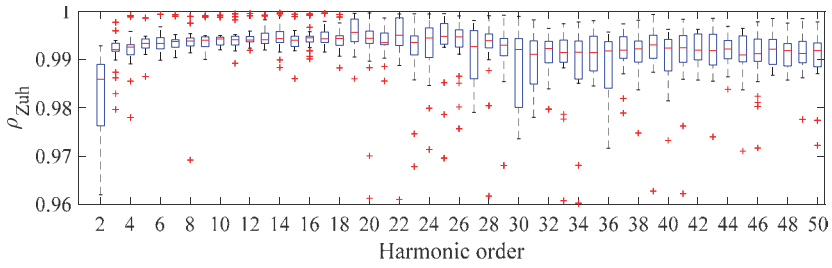
Fig. 12 − *Distribution of the correlation coefficient for the utility impedance depending on the harmonic order.*
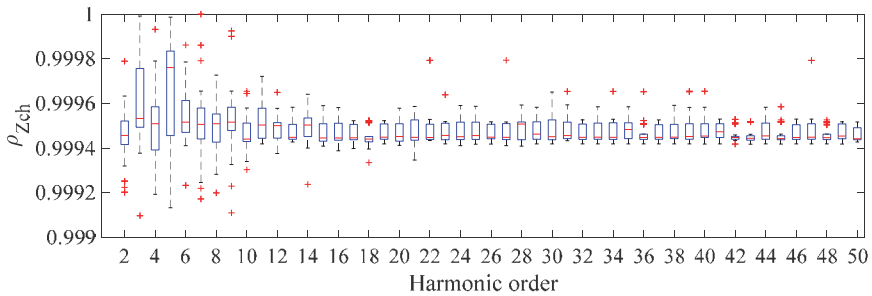

Fig. 13 − *Distribution of the correlation coefficient for the customer impedance depending on the harmonic order.*

(a)

(b)

Fig. 14 – (a) *Distribution of the correlation coefficient for the utility harmonic contribution depending on the harmonic order;* (b) *Distribution of the correlation coefficient for the customer harmonic contribution depending on the harmonic order.*

Due to certain challenges of constructing a DSP-based stimuli generator and reference impedance setup only theoretical assessment of the method's accuracy is discussed in this paper. If complemented with the noise related accuracy analysis previously considered in [17] such theoretical verification can provide an insight in error-prone procedures of the method and finally allow the estimation of its feasibility in lab or real grid conditions.

In fact, parameters of a DSP-based pulse sequence generator, e.g., preset ADC resolution, PWM switching frequency, pulse sequence length and type of the signal conditioning circuit are mostly responsible for the method's inaccuracies in real-life applications [13]. Their effects are not assessed by the present theoretical analysis and will be the topic of the stand-alone paper considering practical implementation of the proposed approach and, in particular, the construction of a prototype of a DSP-based pulse sequence generator.

5   Comparison with Typical Harmonic Identification Methods

This section contains comparison of the proposed approach with typical fluctuation and regression methods. At first short theoretical description of the methods is provided followed by demonstration of their implementation in particular simulation cases.

5.1 Fluctuation method

The fluctuation method [2] utilizes daily variations of voltage and current harmonics at the PCC in order to form arrays of respective increments $\Delta \underline{U}_h$ and $\Delta \underline{I}_h$. A ratio of voltage and current increments corresponding to particular harmonic order allows to define an array of complex impedance that is then distributed between utility and customer, based on the sign of real part of its elements.
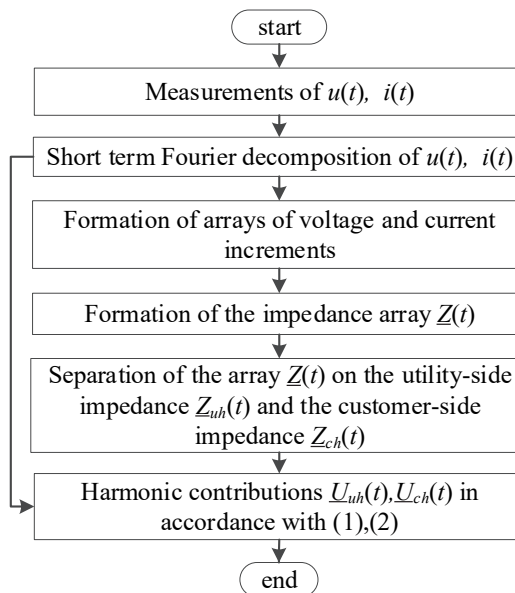

Fig. 15 – *Flow chart of the fluctuation method.*

Defined impedance values enable calculation of harmonic contributions of utility and customer according to (1) and (2). The algorithm of the fluctuation method is presented in the flow chart of Fig. 15.

5.2 Regression method

The partial linear regression method [4] estimates harmonic contributions during the considered period in accordance with the corresponding linear equation:

$$y = D\beta + f , \tag{8}$$

where y and D – matrices of measured real and imaginary values of harmonic voltage and current, f – matrix of real and imaginary values of background harmonic distortion, β – matrix of grid impedance.

start

| Measurements of $u(t)$, $i(t)$ | 1 stage |

Short term Fourier decomposition of $u(t)$, $i(t)$ | 2 stage |

Determining the optimal window width

Formation of a smoothing matrix

Formation of matrices of the current D and voltage y

Calculation biased estimation of the harmonic impedance and background distortion

Formation of complex matrices r и Q

Calculation the unbiased estimation by the complex linear least squares method. Determination of system impedance $\underline{Z}_{it}$

Harmonic contribution $\underline{U}_{ch}(t) = \underline{Z}_{it} \underline{I}_h(t)$
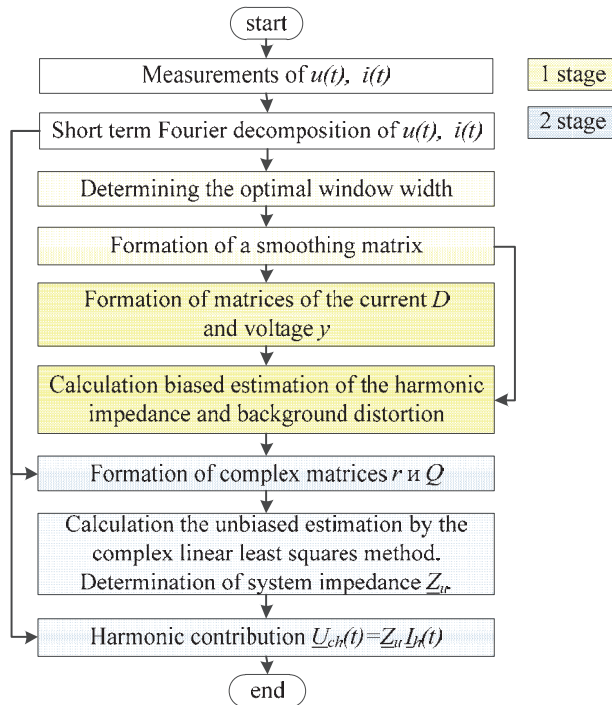
end

Fig. 16 – *Flow chart of the partial linear regression method.*

At the first stage the biased estimation of harmonic impedance and background harmonic distortion are obtained by kernel smoothing estimation method. These parameters are further used to construct a complex linear regression model:

$$r = Q\xi , \tag{9}$$

where Q – matrix of measured current at the PCC; r – matrix of customer harmonic contribution defined as a difference between the values of measured voltage at the PCC and an estimate of background harmonic distortion.

An accurate estimation of harmonic impedance ξ can be calculated from (9) using complex linear least squares method:

$$\xi = (\tilde{Q}'Q)^{-1}\tilde{Q}'r . \tag{10}$$

Finally, harmonic voltage contribution of the customer can be estimated by (6) under the assumption that the customer-side harmonic impedance is much greater than that of the system. The algorithm of the regression method is presented in the flow chart of Fig. 16.

5.3 Harmonic contribution assessment by considered methods

Aforementioned fluctuation and regression methods for harmonic identification were implemented together with the proposed approach into the network simulation model of Fig. 9. The adopted scenario of switching events within the model is described in **Table 2**.

Table 2
Switchings of the topolology of the network simulation Model.

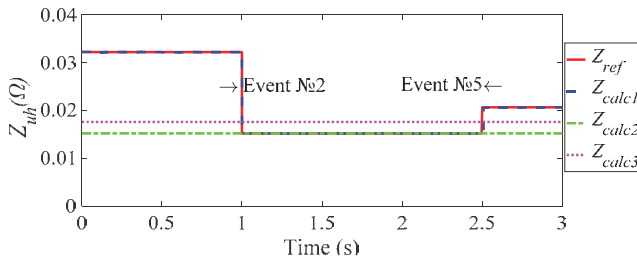| EVENT №	TIME [s]	EVENT
1	0.5	Decrease of background grid harmonic voltage distortion
2	1	Decrease of utility-side impedance
3	1.5	Increase of background harmonic voltage distortion
4	2	Decrease of customer harmonic emission
5	2.5	Increase of utility-side impedance

Fig. 17 – *Comparison of time varying network impedances for the 7th harmonic calculated by the proposed approach (blue line), fluctuation method (green line) and regression method (magenta line) with the reference (red line).*

Hereafter, resulting plots depicting the variation of impedance characteristics (Figs. 17 and 18) and harmonic contributions (Figs. 19 and 20) corresponding to the utility and customer are provided. Each plot contains comparison of the values acquired by the proposed method (blue dashed line), fluctuation (green dash-dot

42

line) and regression methods (magenta dotted line) with the reference (red solid line). As the calculation procedure for different harmonic orders is essentially the same, only the 7th harmonic is presented in the plots for the sake of brevity.

It follows from Fig. 17 that only proposed approach (blue line) recognizes the moderate changes of utility-side impedance. The fluctuation method (green line, Fig. 17) does not identify the variation of the system impedance (green line) probably due to the insufficiency of the corresponding current increments while the regression method (magenta line, Fig. 17) inherently assumes a constant value of the impedance.
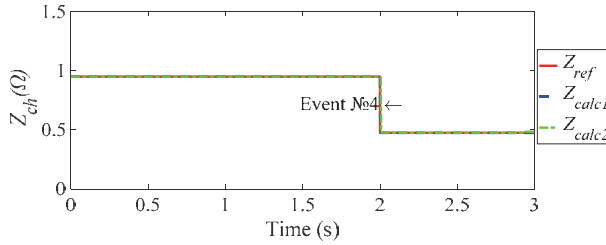

Fig. 18 – *Comparison of time varying customer impedances for the 7th harmonic calculated by the proposed approach (blue line), fluctuation method (green line) with the reference (red line).*

Fig. 19 – *Comparison of the 7th voltage harmonic contributions of considered network calculated by the proposed approach (blue line), fluctuation method (green line) and regression method (magenta line) with the reference (red line).*
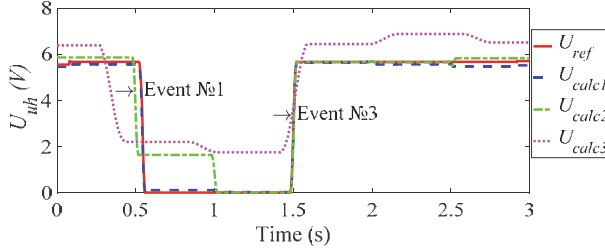

Fig. 20 – *Comparison of the 7th voltage harmonic contributions of considered non-linear load calculated by the proposed approach (blue line), fluctuation method (green line) and regression method (magenta line) with the reference (red line).*
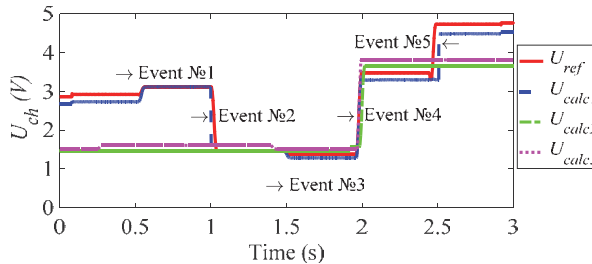
43

The more prominent changes of the customer–side impedance in Fig. 18 are accurately detected by both proposed approach (blue line) and the fluctuation method (green line). The regression method is not able to determine customer-side impedance.

The utility-side harmonic contribution in Fig. 19 is accurately represented by the pulse sequence method over the entire time interval (blue line). The corresponding results of the fluctuation method (green line, Fig. 19) feature relatively good accuracy except for the time interval from 0.5s to 1s with increased error. The regression method (magenta line, Fig. 19) produces the least accurate characteristic of harmonic contribution that generally corresponds to the reference however features significant errors probably due to the nature of kernel smoothing.

Finally, the customer-side harmonic contribution is determined in Fig. 20 most accurately by the pulse sequence method (blue line). Conversely, the results of the fluctuation (green line, Fig. 20) and regression methods (magenta line, Fig. 20) feature significant deviations from the reference in the time intervals from 0 to 1s and from 2.5s to 3s. According to (2) these inaccuracies originate from the errors of produced utility impedance characteristics during the respective time intervals (green and magenta lines, Fig. 17).

Table 3
Customer and Utility Impedances and Harmonic
Contributions Calculated by Considered Methods.

	REFERENCE	FLUCTUATION	PLRM	TERNARY PULSE SEQUENCES
UTILITY-SIDE				
Z_{uh} [Ω]	**0.0217**	0.0152	0.0176	**0.022**
$RMSE_{Zuh}$	-	0.0101	0.0086	**0.0018**
ρ_{Zuh}	-	3.0798e-12	4.1183e-15	**0.9727**
U_{uh} [V]	**3.8623**	4.0296	4.8097	**3.712**
$RMSE_{Uuh}$	-	0.7802	1.4730	**0.1179**
ρ_{Uuh}	-	0.9624	0.9814	**0.9995**
CUSTOMER-SIDE				
Z_{ch} [Ω]	**0.7916**	0.8045	-	**0.796**
$RMSE_{Zch}$	-	0.0229	-	**0.0464**
ρ_{Zch}	-	0.9946	-	**0.9786**
U_{ch} [V]	**2.8780**	2.1528	2.3548	**2.687**
$RMSE_{Uch}$	-	0.9972	0.8912	**0.2417**
ρ_{Uch}	-	0.7606	0.7464	**0.9860**

A quantitative accuracy estimation of the three methods is based on calculation of the root mean squared error (RMSE) and correlation coefficient ρ for impedance and harmonic contribution characteristics. The RMSE is determined as:

$$RMSE = \sqrt{\frac{\sum_{i=1}^{n}(x_i - y_i)^2}{n}} \ , \qquad (11)$$

where x, y are the calculated and reference values respectively.

The results of three methods including mean values of calculated impedances and harmonic contributions, respective RMSE and correlation coefficients for the 7th harmonic are shown in **Table 3**. The lowest values of RMSE correspond to the pulse sequence method, as well as the correlation coefficient close to $0.97 – 0.99$.

6   Discussion of the Results

Modeling results described in the previous sections justify good accuracy of the pulse sequence approach for harmonic identification under non-ideal grid conditions. Network operating mode with varying impedance characteristics, multiple switchings of customer and utility equipment were implemented in the network simulation model in order to emphasize the advantages of the proposed approach for the real-time determination of harmonic contributions under nonstationary grid conditions. Currently adopted approaches for determination of harmonic contributions, e.g., fluctuation or regression methods, turn out to be ineffective due to inherent limitations. For example, the fluctuation method fails to produce accurate results in cases of weak grids or insufficient variations of harmonic levels of the customer. Similarly, the regression method presents low applicability for the assessment of nonstationary operating modes due to the properties of the adopted kernel smoothing techniques.

Conversely, high time resolution and wide frequency range of determined harmonic contributions, flexibility and low invasiveness provided by ternary pulse sequences make their implementation favorable for harmonic source identification in cases of frequently varying loads, weak grids with indistinct sources of distortion or comparable harmonic contributions of utility and customer. The main limitation of the pulse sequence method is the requirement for the generator of the measurement stimuli.

A short summary of aforementioned analysis is given in **Table 4**.

Table 4

Comparison of Considered Approaches for Determination of Harmonic Contributions.

CRITERIA	FLUCTUATION	PLRM	TERNARY PULSE SEQUENCES
Initial Data	Measured voltage and current at the PCC		
Limitations of applicability	Sufficient prominence of harmonic source at any time instant is required	Assumption of constant network harmonic impedance is adopted	Generation of the ternary pulse sequence is required
Complexity	High	High	Low
Determination of varying harmonic contribution over the measurement interval	**Yes**		
Account for varying customer impedance	**Yes**	**No**	**Yes**
Application Area	For nonlinear variable loads	Electric networks, where $Z_{uh} << Z_{ch}$, and also $Z_{uh} = const$	No limits

7   Conclusion

An effective method for the assessment of time-varying harmonic contributions based on the use of the ternary pulse sequence is presented. The verification of the method is produced within time-domain network simulation model including developed white-box model of pulse sequence generator. Comparison with state-of-art approaches for harmonic identification reveals its advantages under non-ideal grid conditions. The real-time capability of the pulse sequence method allows its application in the weak grids featuring frequent topological changes, containing power factor capacitors and significant non-linear loads with abrupt changes of operating modes. Further research will involve development of a prototype of a pulse sequence generator and the analysis of its efficiency in real-life applications.

8   Acknowledgment

9   References

[1]   A. Špelko, B. Blažič, I. Papič, M. Pourarab, J. Meyer, X. Xu, S. Z. Djokic: CIGRE/CIRED JWG C4.42: Overview of Common Methods for Assessment of Harmonic Contribution from Customer Installation, Proceedings of the IEEE Manchester PowerTech Conference, June 2017, Manchester, UK, pp. 1 – 6.

[2]   R. Sinvula, K. M. Abo-Al-Ez, M. T. Kahn: Harmonic Source Detection Methods: A Systematic Literature Review, IEEE Access, Vol. 7, June 2019, pp. 742831 – 674299.

[3]   M. Shojaie, H. Mokhtari: A Method for Determination of Harmonics Responsibilities at the Point of Common Coupling Using Data Correlation Analysis, IET Generation, Transmission and Distribution, Vol. 8, No. 1, January 2014, pp. 1421 – 6150.

[4]   H. Hua, Z. Liu, X. Jia: Partially Linear Model for Harmonic Contribution Determination, IEEJ Transactions on Electrical and Electronic Engineering, Vol.11, No. 3, May 2016, pp. 2851 – 6291.

[5]   E. Gursoy, D. Niebur: Harmonic Load Identification Using Complex Independent Component Analysis, IEEE Transactions on Power Delivery, Vol. 24, No. 1, January 2009, pp. 2851 – 6292.

[6]   K. K. C. Yu, N. R. Watson, J. Arrillaga: An Adaptive Kalman Filte for Dynamic Harmonic State Estimation and Harmonic Injection Tracking, IEEE Transactions on Power Delivery, Vol. 20, No. 2, April 2005, pp.15771 – 61584.

[7]   A. Y. Hatata, M. Eladawy: Prediction of the True Harmonic Current Contribution of Nonlinear Loads Using NARX Neural Network, Alexandria Engineering Journal, Vol. 57, No. 3, September 2018, pp. 15091 – 61518.

[8]   F. Safargholi, K. Malekian, W. Schufft: On the Dominant Harmonic Source Identification – Part I: Review of Methods, IEEE Transactions on Power Delivery, Vol. 33, No. 3, June 2018, pp. 12681 – 61277.

[9]   T. Zang, Z. He, Y. Wang, L. Fu, Z. Peng, Q. Qian: A Piecewise Bound Constrained Optimization for Harmonic Responsibilities Assessment under Utility Harmonic Impedance Changes, Energies, Vol. 10, No. 7, July 2017, pp. 11 – 620.

[10] A. H. Tan, K. R. Godfrey: The Generation of Binary and Near-Binary Pseudorandom Signals: An Overview, IEEE Transactions on Instrumentation and Measurement, Vol. 51, No. 4, August 2002, pp. 5831 – 6588.

[11] Md. A. Ali, E. Ali, Md. A. Habib, Md. Nadim, T. Kusaka, Y. Nogami: Pseudo Random Ternary Sequence and its Autocorrelation Property over Finite Field, International Journal of Computer Network and Information Security, Vol. 11, No. 9, September 2017, pp. 541 – 663.

[12] A. De Angelis, J. Schoukens, K. R. Godfrey, P. Carbone: Practical Issues in the Synthesis of Ternary Sequences, IEEE Transactions on Instrumentation and Measurement, Vol. 66, No. 2, February 2017, pp. 2121 – 6222.

[13] T. Roinila, T. Messo: Online Grid-Impedance Measurement Using Ternary-Sequence Injection, IEEE Transactions on Industry Applications, Vol. 54, No. 5, September 2018, pp. 50971 – 65103.

[14] H. E. Mazin, W. Xu, B. Huang: Determining the Harmonic Impacts of Multiple Harmonic-Producing Loads, IEEE Transactions on Power Delivery, Vol. 26, No. 2, April 2011, pp. 11871 – 61195.

_

[15] L. Hassaine, E. OLias, J. Quintero, V. Salas: Overview of Power Inverter Topologies and Control Structures for Grid Connected Photovoltaic Systems, Renewable and Sustainable Energy Reviews, Vol. 30, February 2014, pp. 7961 – 6807.

[16] M. Ciobotaru, T. Kerekes, R. Teodorescu, A. Bouscayrol: PV Inverter Simulation Using MATLAB/Simulink Graphical Environment and PLECS Blockset, Proceedings of the 32nd Annual Conference on IEEE Industrial Electronics (IECON2006), Paris, France, November 2006, pp. 53131 – 65318.

[17] E. Bulycheva, S. Yanchenko: Online Determination of Varying Harmonic Load Contribution to Grid Voltage Distortion, Proceedings of the International Conference on Industrial Engineering, Applications and Manufacturing (ICIEAM), Sochi, Russia, May 2020, pp. 11 – 66.